Application of 3D reconstruction system in diabetic foot ulcer injury assessment

Cite as: AIP Conference Proceedings **1955**, 040119 (2018); https://doi.org/10.1063/1.5033783
Published Online: 18 April 2018

Jun Li, Li Jiang, Tianjian Li, et al.

Application of 3D reconstruction system in diabetic foot ulcer injury assessment

Jun Li[a)], Li Jiang[b)], Tianjian Li, Xiaoyao Liang

School of Electronic Information and Electrical Engineering, Shanghai Jiao Tong University
Shanghai, China

a) lijun1532@sjtu.edu.cn
b) ljiang_cs@sjtu.edu.cn

Abstract. To deal with the considerable deviation of transparency tracing method and digital planimetry method used in current clinical diabetic foot ulcer injury assessment, this paper proposes a 3D reconstruction system which can be used to get foot model with good quality texture, then injury assessment is done by measuring the reconstructed model. The system uses the Intel RealSense SR300 depth camera which is based on infrared structured-light as input device, the required data from different view is collected by moving the camera around the scanned object. The geometry model is reconstructed by fusing the collected data, then the mesh is sub-divided to increase the number of mesh vertices and the color of each vertex is determined using a non-linear optimization, all colored vertices compose the surface texture of the reconstructed model. Experimental results indicate that the reconstructed model has millimeter-level geometric accuracy and texture with few artificial effect.

Key words: Diabetic Foot Ulcer; 3D reconstruction; depth camera.

INTRODUCTION

Diabetic foot ulcer is a complicated disease caused by long-term increase in blood sugar, often results in ulcer below the ankle, ischemia, deformity and necrosis. The prognosis of diabetic foot ulcer is affected by many factors, the more intuitive area and depth of ulcer are important judgment criteria standards of prognosis [1]. The transparency tracing method is most used before the development of digital imaging technology, it is difficult to operate, has poor accuracy and is easy to form cross-contamination [2]. The application of 2D digital imaging software increases the estimate accuracy of ulcer area and decreases the complexity of operation [3]. The wound volume is also increasingly being estimated with the help of digital images and photogrammetric software, e.g. VeVMD (Vista Medical, Winnipeg, Manitoba, Canada)[4]. Due to the limitations of 2D images, those software are heavily influenced by the fold back plane and irregular shape of ulcer, which causes the resulting error to be hard to correct. Especially, measurements based on two-dimensional images are powerless to deal with ulcer depth and depth gradient changes. At the same time, the clinical application of 3D human body scan measurement technology has been studied in neurosurgery [5], foot health [6] and so on. This new technology is expected to have good application in the measurement of area, volume and characteristic of diabetic foot ulcer.

Scene reconstruction has always been a hot research field in computer vision. Some methods directly compute the scene depth information from RGB images [7] [8], which have high requirements at the scene surface material and lighting and cannot guarantee better accuracy. Recently the appearance of depth camera, like Microsoft Kinect, provides a new possibility for dense 3D reconstruction. The KinectFusion algorithm [9], proposed by Newcombe et al, has proved the feasibility of 3D reconstruction system based on RGB-D camera using TSDF (truncated signed distance function) as fusion media. In KinectFusion the tracking of depth camera pose is accomplished using ICP (Iterative Closest Point) algorithm [11]. After all frames have been fused in the TSDF volume, the mesh of the scene

Advances in Materials, Machinery, Electronics II
AIP Conf. Proc. 1955, 040119-1–040119-8; https://doi.org/10.1063/1.5033783
Published by AIP Publishing. 978-0-7354-1654-3/$30.00

can be extracted using MarchingCubes algorithm [12]. In recent years many more algorithm [13][14] have been developed to expand the application of RGB-D 3D reconstruction.

OVERVIEW

Our 3D scanning system consists of a depth camera and auxiliary drive system. Fig. 1 is a schematic view of the drive system. A screw guide allows the camera to move horizontally. A stepping motor drives the camera to rotate in the horizontal direction. The whole system is in a circular motion in the vertical plane driven by another motor. With the help of those motors, the system can complete the entire multi-angle scan data acquisition in about 20 seconds. Compared to hand-held scanning method, using motor to drive the camera can reduce the noise of depth frame and blurring of RGB frame caused by hand jitter, greatly improving the accuracy of the data collected.

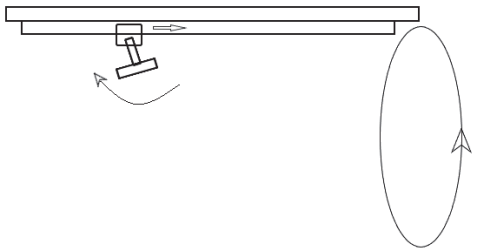

FIGURE 1 Schematic view of the drive system

In recent years the appearance of active depth camera using near infrared band light source, have greatly reduced the cost and complexity of simultaneously obtaining the depth and lighting information of the scene. This led us to choose the infrared depth camera as the input device. Based on the principle of depth acquisition, infrared depth camera can be further divided into Time of Flight (ToF) and structured light. ToF-based depth cameras calculate the scene depth information by measuring the propagation delay or phase difference of the light pulses between being transmitted and being reflected from the object to the receiving sensor. Structured light-based depth cameras use optical encoding technology to determine the scene depth information by projecting a predefined infrared pattern to the scene and capturing the deformation of the pattern. Table 1 lists the most common infrared depth cameras and their parameters. To increase the resolution of the depth map in the imaging plane, the device should have higher depth map resolution and smaller effective distance. Taken together, the Intel RealSense SR300 is chosen as the data acquisition device in our reconstruction system.

The reconstruction algorithm used in our system consists of geometric model reconstruction and surface texture generation. In the geometric model reconstruction section, the RGB-D stream obtained from the depth camera is used to reconstruct the mesh of the scanned object. In the surface texture generation section, we first subdivide the mesh obtained in the previous section to increase the mesh vertex count. Then an appropriate number of RGB images with high quality selected from the RGB-D stream are used to determine the color for each vertex in the subdivided mesh by non-linear optimization. The color of all the vertices make up the surface texture of the scanned object.

GEOMETRIC RECONSTRUCTION

The geometric model reconstruction algorithm used in our system is based on the algorithm proposed in [13]. The process is shown in Fig. 2.

Camera Pose Estimation

The camera pose can be represented as the 6-dimensiona twist coordinates

$$\xi=\left(\omega_1,\omega_2,\omega_3,v_1,v_2,v_3\right), \tag{1}$$

where (ν_1, ν_2, ν_3) represents the translational components and $(\omega_1, \omega_2, \omega_3)$ the rotational components. T_ξ is the corresponding pose matrix of ξ . We use function D to represent the depth map

$$D: \Re^2 \to \Re, \tag{2}$$

and function V to represent the TSDF volume

$$V: \Re^3 \to \Re. \tag{3}$$

TABLE I. COMMONLY USED INFRARED DEPTH CAMERAS

Device	**Parameters**		
	Depth resolution	***Effective distance***	***Principle***
Microsoft Kinect V1	320x240	0.4-4.5m	Structured light
Microsoft Kinect V2	512x424	0.5-4.5m	ToF
ASUS Xtion pro	640x480	0.8-3.5m	Structured light
Intel Realsense SR300	640x480	0.3-2m	Structured light

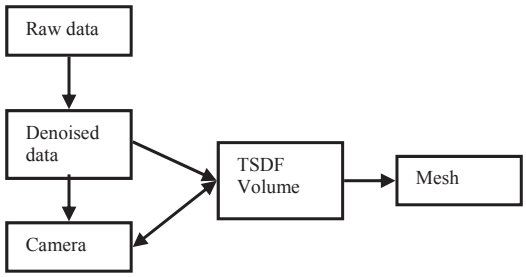

FIGURE 2 Process of the geometric reconstruction algorithm

Reference [13] also proposed a new weight choosing scheme to update the TSDF volume

$$\omega(d) = \begin{cases} 1 & |d| < \varepsilon \\ e^{-\sigma(|d|-\varepsilon)^2} & |d| \geq \varepsilon, |d| \leq \delta \\ 0 & |d| \geq \delta \end{cases}, \tag{4}$$

where *d* refers to the distance value, δ to the TSDF truncation distance and ε to a distance threshold determined by the characteristics of the depth camera. ε should be smaller than δ. With function π representing the projection from image space to camera space, the vertex ***v*** corresponding to a pixel ***p*** in the depth map can be described as

$$v_p = \pi(p, D(p)). \tag{5}$$

The energy function is defined as

$$\mathrm{E} = \sum_{p} \left(V\left(T_{\xi} v_{p} \right) \right)^{2} . \tag{6}$$

The desired pose is

$$\xi = \arg\min_{\xi} E . \tag{7}$$

This is also the most significant difference between the algorithm proposed by [13] and the KinectFusion algorithm.

3D Printing

To quantitatively analyze the accuracy of 3D reconstruction algorithm, we made a foot model with known size using 3D printing. The reconstruction result of the printed model can be used to determine the accuracy by comparing it with the original mesh. It is less expensive compared with using high precision industrial scanner to obtain the ground truth. We also noticed that the technology and materials used in 3D printing will have a great influence on the depth data obtained by the camera due to the different reflection characteristics of the infrared light. The thickness of the printed model is also a very important factor. We use Stereo Lithography Appearance (SLA) and UV Curable Resin with 2mm thickness. Fig 3 shows the object model which we used in this paper.

Two Stage Reconstruction

We found that different value of ε and δ will influence the accuracy of camera pose estimation and smoothness of the resulting mesh. To tolerate the noise of depth map, we need larger values in the camera pose estimation stage , which also causes the result to be too smooth at the edges, especially between the toes. In response to this problem, we propose a two-stage tracking reconstruction method. After the camera poses of each frame have been determined, we fuse all the frames to a new TSDF volume with different weighting function parameters, which will result in a 3D model with sharper edge.

SURFACE TEXTURE GENERATION

There are two traditional methods to generate surface texture for models reconstructed using RGB-D depth camera. First one is to map each triangle of the reconstructed mesh to a RGB image and synthesize each mapped region into one texture map [16]. Another one is to subdivide the mesh and determine the color value for each vertex of the subdivided mesh, the surface texture is saved in the form of all vertices' color implicitly [17]. The texture generation algorithm used in this paper is based on [17].

Texture Generation Algorithm

Fig. 4 represents the basic flow of the texture generation algorithm. In the mesh subdividing stage, each triangle of the mesh is divided into four sub-triangles using the middle points of the three edges [18]. The subdivision can increase the number of vertices without geometrical change to the mesh. Next is the keyframe selection stage. Proposed algorithm selects proper keyframes based on the image blurring degree [19] and camera pose of each image from the RGB-D stream. The selected keyframes are further used in a global non-linear optimization to generate the texture. In the global optimization stage, the camera poses and image deformation of each keyframe are adjusted to get clear and sharp textures. Finally, each vertex is assigned to several keyframes with appropriate weights which are used to compute the vertex color as a weighted average. Fig.5 represents texture results generated by the geometry reconstruction algorithm. Fig. 6 represents the results after texture generation optimization.

Supplementary lighting

Since the algorithm is strongly depends on the assumption that the color values of the same point are constant among keyframes obtained from different view, the lighting conditions have great impact on the performance of the algorithm. To get adequate lighting at all scanning views, we provide many fill lights. It should be noted that all light should avoid the near-infrared band to eliminate impacts on depth camera.

FIGURE 3. The test object model

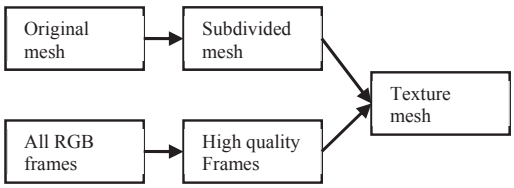

FIGURE 4. Process of the texture Generation Algorithm

FIGURE 5 The blended texture from geometry reconstruction

FIGURE 6. Texture after optimization

EXPERIMENT RESULTS AND ANALYSIS

We implemented the geometry reconstruction and texture generation algorithm by ourselves according to [13][17] with the help of the opensource Point Cloud Library (PCL) [20]. The implemented software is further improved using CUDA(Compute Unified Device Architecture) framework to take full advantage of the high parallel computing power of modern GPGPU(General Purpose Graphics Processing Unit). As for reconstruction error analysis, we use the Hausdorff distance metric[21] implemented by MeshLab[12].

The algorithms are tested on a personal computer with Intel core i5 CPU and Nvidia GTX 1060 GPU. The scanning phase took about 20 seconds at 30 frames per second, resulting in approximate 600 RGB-D frames. The two-stage geometry reconstruction section cost 18 seconds. The texture generation section cost 5 minutes with 80 optimization iterations.

For the two-stage reconstruction algorithm, we set ε to 2mm and δ to 9mm for the first stage, ε to 1mm and δ to 6mm for the second stage. Fig. 7 and Fig. 8 represent the reconstruction results of the 3D-printed model for each stage. It can be observed that the margin of toes is sharper in Fig. 8. Fig. 9 represents the error distribution results of original test model for both stages. The second stage can improve the reconstruction error as shown in Fig.9. Fig.10 represents the actual reconstruction result for a foot of volunteer.

FIGURE 7. One stage reconstruction result

FIGURE 8. Two stage reconstruction result

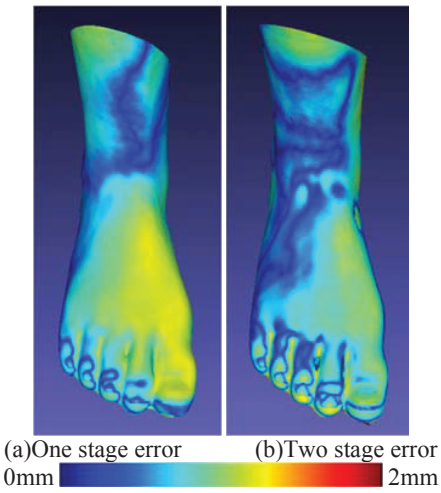

FIGURE 9. The error distribution of one and two stage results

FIGURE 10. The reconstruction result of a real foot

CONCLUSION

In this paper, we propose a 3D scanning reconstruction system suitable for the injury assessment of diabetic foot ulcer. The system uses an infrared structured light depth camera as input device, captures the needed data from different views by driving the depth camera with motors. After geometric reconstruction several RGB images with less blurring are chosen to generate the model surface texture by non-linear optimization. The experimental results show that the system can reconstruct with millimeter-level geometric accuracy and texture with few artificial effect. Based on the reconstructed model, automatic ulcer location and measurement algorithm can be studied considering the characteristics of diabetic foot ulcer.

REFERENCES

1. L. A. Lavery, S. A. Barnes, M. S. Keith, J. W. Seaman and D. G. Armstrong, "Prediction of Healing for Postoperative Diabetic Foot Wounds Based on Early Wound Area Progression," Diabetes Care, vol. 31, pp. 26-29, 2008.
2. G. Gethin and S. Cowman, "Wound measurement comparing the use of acetate tracings and VisitrakTM digital planimetry,"Journal of Clinical Nursing, vol. 15, pp. 422-427, 2006.
3. R. Shetty, H. Sreekar, S. Lamba and A. K. Gupta, "A novel and accurate technique of photographic wound measurement," Indian Journal of Plastic Surgery, vol. 45, p. 425, 2012.
4. S. E. Gardner, R. A. Frantz, S. L. Hillis, T. J. Blodgett, L. M. Femino and S. M. Lehman, "Volume Measures Using a Digital Image Analysis System are Reliable in Diabetic Foot Ulcers," Wounds-a Compendium of Clinical Research and Practice, vol. 24, pp. 146-151, 2012.
5. Y. Fan, D. Jiang, M. Wang and Z. Song, "A new markerless patient-to-image registration method using a portable 3D scanner," Medical Physics, vol. 41, p. 101910, 2014.
6. M. Saghazadeh, N. Kitano and T. Okura, "Gender differences of foot characteristics in older Japanese adults using a 3D foot scanner," Journal of Foot and Ankle Research, vol. 8, pp. 29-29, 2015.
7. D. Scharstein, R. Szeliski and R. Zabih, "A taxonomy and evaluation of dense two-frame stereo correspondence algorithms," International Journal of Computer Vision, vol. 47, pp. 7-42, 2001.
8. H. Hirschmuller, "Stereo Processing by Semiglobal Matching and Mutual Information," IEEE Transactions on Pattern Analysis and Machine Intelligence, vol. 30, pp. 328-341, 2008.
9. R. A. Newcombe, S. Izadi, O. Hilliges, D. Molyneaux, D. Kim and A. J. Davison, "KinectFusion: Real-time dense surface mapping and tracking," International symposium on mixed and augmented reality, 2011.
10. B. Curless and M. Levoy, "A volumetric method for building complex models from range images," International conference on computer graphics and interactive techniques, 1996.
11. T. Whelan, H. Johannsson, M. Kaess, J. J. Leonard and J. Mcdonald, "Robust real-time visual odometry for dense RGB-D mapping," International conference on robotics and automation, 2013.
12. R. A. Newcombe, D. Fox and S. M. Seitz, "DynamicFusion: Reconstruction and tracking of non-rigid scenes in real-time," Proceedings of the IEEE conference on computer vision and pattern recognition, 2015.
13. E. Bylow, "Real-Time Camera Tracking and 3D Reconstruction Using Signed Distance Functions," Robotics science and systems, 2013.
14. P. J. Besl and H. D. Mckay, "A method for registration of 3-D shapes," IEEE Transactions on Pattern Analysis and Machine Intelligence, vol. 14, no. 2, pp. 239-256, 1992.
15. W. E. Lorensen and H. E. Cline, "Marching cubes: A high resolution 3D surface construction algorithm," International conference on computer graphics and interactive techniques, vol. 21, pp. 163-169, 1987.
16. J. Jeon, Y. Jung, H. Kim and S. Lee, "Texture map generation for 3D reconstructed scenes," The Visual Computer, vol. 32, pp. 955-965, 2016.
17. Q. Zhou and V. Koltun, "Color Map Optimization for 3D Reconstruction with Consumer Depth Cameras," in International conference on computer graphics and interactive techniques, 2014.
18. J. Peters and U. Reif, "The simplest subdivision scheme for smoothing polyhedra," ACM Transactions on Graphics, vol. 16, pp. 420-431, 1997.
19. F. Crete, T. Dolmiere, P. Ladret and M. Nicolas, "The Blur Effect: Perception and Estimation with a New No-Reference Perceptual Blur Metric," Proceedings of SPIE, 2007.
20. R. B. Rusu and S. Consins, "3D is here: Point Cloud Library (PCL)," in International conference on robotics and automation, 2011.
21. M. Dubuisson and A. K. Jain, "A modified Hausdorff distance for object matching," in International conference on pattern recognition, 1994.
22. P. Cignoni, M. Callieri, M. Corsini, M. Dellepiane, F. Ganovelli and G. Ranzuglia, "MeshLab: an Open-Source Mesh Processing Tool," in Eurographics Italian Chapter Conference, 2008.